Fluid transport in branched structures with temporary closures: A model for quasistatic lung inflation

Arnab Majumdar,[1,2] Adriano M. Alencar,[1,2] Sergey V. Buldyrev,[1] Zoltán Hantos,[3] H. Eugene Stanley,[1] and Béla Suki[2]

[1]*Center for Polymer Studies and Department of Physics, Boston University, Boston, Massachusetts 02215*
[2]*Department of Biomedical Engineering, Boston University, Boston, Massachusetts 02215*
[3]*Department of Medical Informatics and Engineering, and Institute of Surgical Research, University of Szeged, Hungary*

We analyze the problem of fluid transport through a model system relevant to the inflation of a mammalian lung, an asymmetric bifurcating structure containing random blockages that can be removed by the pressure of the fluid itself. We obtain a comprehensive description of the fluid flow in terms of the topology of the structure and the mechanisms which open the blockages. We show that when calculating averaged flow properties of the fluid, the tree structure can be partitioned into a linear superposition of one-dimensional chains. In particular, we relate the pressure-volume P-V relationship of the fluid to the distribution $\Pi(n)$ of the generation number n of the tree's terminal branches, a structural property. We invert this relation to obtain a statistical description of the underlying branching structure of the lung, by analyzing experimental pressure-volume data from dog lungs. The $\Pi(n)$ extracted from the experimental P-V data agrees well with available data on lung branching structure. Our general results are applicable to any physical system involving transport in bifurcating structures with removable closures.

I. INTRODUCTION

The complex structure of biological systems [1–6] and transport processes that occur in them [7–13] are topics of much current interest, attracting researchers from engineering [14–16], physics [17–20], and physiology [21–23]. In this paper, we address the problem of forcing fluid through an asymmetrically branched structure with random closures that can be removed by the pressure of the fluid. Such problems are often encountered during fluid flow in organ systems where the pathways can be blocked, e.g., circulation of blood [21] and flow of air in the lung [24,25]. Unrestricted flow in these pathways is essential for proper physiological function, and blockages lead to potentially lethal situations. In spite of its critical application, the problem of fluid flow through collapsible bifurcating structures has only been marginally studied [26–29]. Recently, we introduced a simple tree model to characterize the asymmetry of the lung airway tree using pressure-volume curves during inflation [30]. Here we propose a general method to obtain analytical results for tree structures and apply it to the process of lung inflation.

The primary function of the respiratory systems is to deliver air to the air sacs, called alveoli, for gas exchange. Morphological data show that the mammalian lung consists of airways arranged hierarchically in an asymmetric binary tree, the airway tree, with air sacs connected to the terminals [31,32]. Many peripheral airways of a diseased lung collapse during expiration as the internal air pressure and the tension of the elastic walls are insufficient to counter the surface tension of the liquid lining [33–35]. The liquid forms a bridge or closure (Fig. 1) which completely blocks the flow of air, excluding a large number of alveoli from gas exchange [25]. During inspiration, the difference between the atmospheric pressure and the pressure surrounding the lung, the transpulmonary pressure P is slowly increased. As a result, a pressure difference builds across the closures which are exposed to the atmospheric pressure through the root of the tree. Each closure reopens when the pressure difference across it reaches its critical opening threshold [36,37]. Since the airways are arranged in a tree structure, opening one branch is not possible until all branches connecting it to the root of the tree are open. If the threshold pressure of a daughter branch is smaller than that of its parent, the daughter opens simultaneously with the parent. This mechanism also applies to subsequent generations, leading to avalanches of airway openings [38].

The process of airway opening via avalanches has been studied for symmetric binary tree models. The volume of inhaled air V during inspiration, for a fully collapsed lung, was found to follow a simple power law in P,

$$V(P) \propto P^N, \tag{1}$$

where N is the generation number of the terminal branches [26–28]. Such pressure-volume (P-V) relations are used to measure lung function in clinical environments. However, the real lung is asymmetric, with many branches missing, which significantly distorts the P-V curve from the ideal power-law behavior [30–32]. It is thus important to determine how the properties of the system depend on the asym-
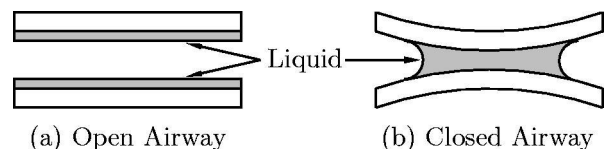

FIG. 1. Section of an airway showing (a) the film of liquid when the airway is open, and (b) the liquid bridge blocking the flow of air when the airway is closed.

metry of its underlying tree structure. Avalanches are further complicated since the opening of an airway is accompanied by an audible pressure wave called crackle [39–41], which in turn can assist the opening of airways downstream. Moreover, the air sacs are elastic and the effect of their elasticity on the P-V curve becomes significant near the end of the inspiratory cycle, when the majority of air sacs have been opened [27]. Although asymmetry, crackles, and elasticity are important contributors to the shape of the P-V curve, their effects are isolated to different regions and thus it is possible to extract information about them by analyzing the same P-V curve.

We obtain experimental P-V curves of isolated dog lung lobes (Sec. II) and develop a model of the lung during avalanchelike airway openings (Sec. III A). We show that when calculating the P-V relationship, it is possible to partition the complex bifurcating structure into a set of paths connecting the root of the structure to the air sacs (Sec. III B). Consequently,

$$V(P) = V_E(P) \sum_n \Pi(n) \Gamma_n(P), \quad (2)$$

where $V_E(P)$ is the elastic P-V relationship of the lung (Sec. II), $\Pi(n)$ is the distribution of terminals with generation number n, and $\Gamma_n(P)$ is the opening probability of an airway of generation n under the influence of avalanches and crackles (Sec. IV).

Using the analytic results of our models, we are able to fit the experimental P-V data (Sec. V) and obtain the distribution $\Pi(n)$, which is a key morphologic property of the airway tree. Since experiments measuring P-V curves of an inflating lung are noninvasive, this method provides a way to study "microscopic" branching structures from "macroscopic" P-V data without the use of invasive techniques [30]. We compared these results with known morphological data on the lung structure. The agreement of our model with experimental data provides a better understanding of both the general problem of fluid flow through blocked pathways and the particular manifestation of this system in the case of the lung.

II. EXPERIMENTAL DATA

We determine experimentally the P-V curves of two isolated dog lung lobes, labeled A and B. A cannula is inserted into the main bronchus and the lobe is degassed in a vacuum chamber as described by Smith and Stamenović [42], collapsing almost all the airways. The degassed lobes are placed in an airtight chamber with the cannula attached to a metal tube that is led through the lid of the chamber, as shown in Fig. 2. We inflate the lobes from the collapsed state to total lobe capacity by steadily decreasing the chamber pressure P_c using a suction pump. We measure the transpulmonary pressure
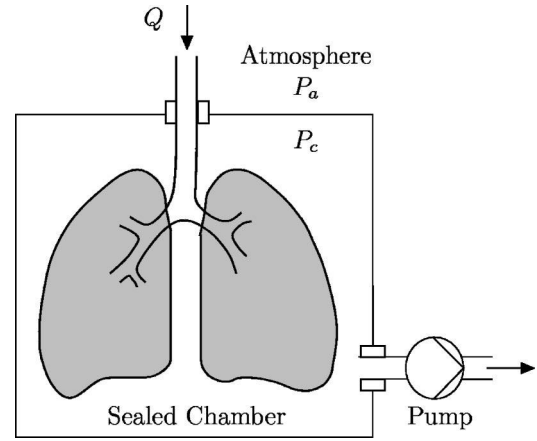
$$P \equiv P_a - P_c$$

FIG. 2. Schematic diagram of the experimental setup. The lobe is placed in a sealed chamber (pressure P_c) with the main bronchus open to the atmospheric pressure P_a. The air pressure in the chamber is slowly decreased using a vacuum pump which creates a pressure difference $P = P_a - P_c$.

by recording the chamber pressure P_c with respect to atmospheric pressure P_a using a Valydine MP-45 transducer (50 cm H_2O). The airflow Q is measured at the main bronchus using a screen pneumotachometer (resistance 5 cm H_2O/l/s) attached to another Validyne MP-45 transducer (2 cm H_2O). Pressure and airflow are both sampled at a rate of 80 Hz. The pressure P is increased to 30 cm H_2O in 120 s. At this inflation rate, the time to regain equilibrium after an airway opens is negligible compared to the total inflation time. The volume V of inhaled air is calculated by integrating Q with respect to time,

$$V(t) = \int_0^t Q(t') dt'. \quad (3)$$

The measured P-V curves are shown in Fig. 3. Although the two lobes have slightly different V at maximum P, both curves show certain common features:

Region A ($P < 10$ cm H_2O): As P increases, V increases only slightly. At these pressures almost all air sacs are collapsed and the slight increase in V is due to the opening of a small number of airways and their subsequent elastic expansion.

Region B (10 cm $H_2O < P < 20$ cm H_2O): Over this range of P, V increases dramatically from near 0 to near saturation. In this region, air sacs are recruited in avalanches giving rise to the steep increase in V.

Region C ($P > 20$ cm H_2O): In this region, almost all air sacs are open and V increases as a result of the elastic expansion of the opened air sacs. We fit this region using a single exponential model for the P-V relation for the elastic expansion of the air sacs [43–45], where $V_E(P)$, the elastic volume of the lung, is given by

$$V_E(P) = V_0(1 - a e^{-bP}), \quad (4)$$

where the parameters V_0, a, and b were determined by fitting experimental data for $P > 20$ cm H_2O and are consistent with those previously obtained [46].
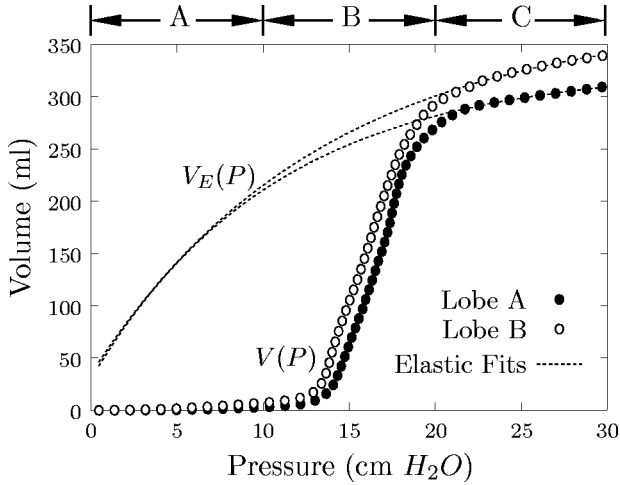
FIG. 3. Experimentally determined P-V curves of two isolated dog lung lobes A ($\bullet$) and B ($\circ$), obtained during inflation from collapsed state to total lobe capacity. The dashed lines show asymptotic fits to $V_E(P)$ given by Eq. (4) with $V_0 = 327.3$ ml, $a = 0.907$, $b = 0.094$/cmH$_2$O for lobe A and $V_0 = 377.1$ ml, $a = 0.908$, $b = 0.075$/cmH$_2$O for lobe B.

When all airways and air sacs in the lung are open, V increases only due to elastic expansion and Eq. (4) describes the P-V curve. If only a fraction f_v of the total volume is open, the P-V curve can be written as

$$V(P) = f_v(P) V_E(P). \qquad (5)$$

Thus, the volume fraction f_v of the open region of the lung can be calculated as

$$f_v(P) = \frac{V(P)}{V_E(P)}, \qquad (6)$$

and is shown in Figs. 4(a) and 4(b) for the lobes A and B.

The total volume V is the sum of the volume contained in the open air sacs, V_a, and the volume contained in the opened airways (branches), V_b,

$$V = V_b + V_a. \qquad (7)$$

In region A, $V_a \approx 0$ as nearly all air sacs are closed and the observed volume $V \approx V_b$. In the fully open lung, region C, when all air sacs are open, V_a is much greater than V_b. This
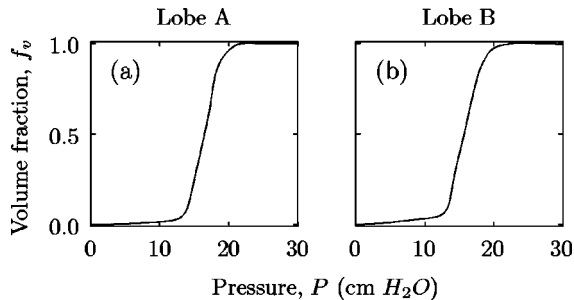

FIG. 4. Volume fraction $f_v(P)$ of the open region of lobes (a) A and (b) B, as defined by Eq. (6).
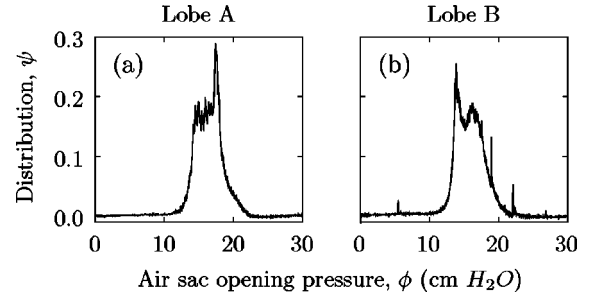

FIG. 5. Distribution $\psi(\phi)$ of opening pressures ϕ of the air sacs in lobe (a) A and (b) B, obtained by differentiating Figs. 4(a) and 4(b) respectively, according to Eq. (9).

approximation is also valid for most of region B, once the first few avalanches occur. We assume that $V_b \ll V_a$ and thus $V \approx V_a$ over the entire range of P; the approximation is more accurate for higher P. If all air sacs are identical and each open air sac contributes an equal volume, the increase in f_v is due to the increase in the fraction of open air sacs f_a,

$$f_v \approx f_a. \qquad (8)$$

As P increases, more air sacs open and contribute to V. The increase in f_v is not continuous, but occurs in steps of different sizes, corresponding to avalanches which recruit varying numbers of contributing air sacs. The opening pressure ϕ of an air sac is defined as the pressure at which the air sac reopens. The distribution $\psi(\phi)$ of opening pressures ϕ is an important measure of lung condition, often used to determine the applied pressures during recruitment maneuvers [47,48] and artificial ventilation [49,50]. When the pressure is increased from P by an amount dP, the increase in the fraction of open air sacs df_a is the fraction of air sacs with opening pressures $\phi \in [P, P + dP]$. Thus the distribution $\psi(\phi)$ can be estimated as

$$\psi(\phi) = \left. \frac{df_a}{dP} \right|_{P=\phi} \approx \left. \frac{df_v}{dP} \right|_{P=\phi}, \qquad (9)$$

using the approximation of Eq. (8). The obtained distributions are shown in Figs. 5(a) and 5(b) for lobes A and B, respectively. Similar distributions of opening pressures have been obtained using computed tomography [51].

III. LUNG INFLATION MODEL

We now develop a model of the P-V curve of an asymmetrically branched tree during inflation. A tree is a minimally connected graph with one and only one path between any two points [52,53]. The lack of redundant paths makes tree structures vulnerable to edge disruptions, since the removal of any one edge affects a large number of paths, significantly affecting the connectivity of the structure. Although this property is the primary cause of many obstructive lung diseases, we can exploit the strong signature of a collapsed airway on macroscopic measurables such as the P-V curve to estimate the connectivity of the tree. Using a simple thresholding model, we first obtain the fraction f_a
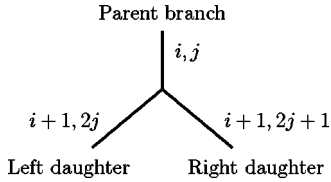
FIG. 6. Convention for labeling branches of the tree according to Eq. (10).

of air sacs open at any pressure P and subsequently an expression of the P-V curve in terms of the tree structure.

A. Binary tree model

To study the inflation through the asymmetric lung, we construct an incomplete binary tree $\mathcal{T}$, defined as a set of branches (airways). Each branch in $\mathcal{T}$ is labeled by a pair of indices (i,j), where the index i is the generation number of the branch and the index j is used to distinguish between branches of the same generation $(0 \leqslant j < 2^i)$. The root of the tree is labeled $(0,0)$.

A branch either bifurcates into two daughters or subtends an air sac. The daughters (i',j') of a bifurcating branch (i,j) are given by

$$(i',j') \equiv \begin{cases} (i+1,2j) & \text{left daughter} \\ (i+1,2j+1) & \text{right daughter,} \end{cases} \quad (10)$$

as shown in Fig. 6. Branches which subtend an air sac are the terminal branches or "leaves" of the airway tree (branches with underlined labels in Fig. 7). The set of all leaves of $\mathcal{T}$ is defined as $\mathcal{L}$, where $\mathcal{L} \subset \mathcal{T}$.

We define a path $\mathcal{P}_{i,j}$ for a branch (i,j) as the set of branches connecting (i,j) to the root of the tree (double line in Fig. 7). We note that according to the definition in Eq. (10), the parent of (i,j) is given by $(i-1,[j/2])$, where $[x]$ represents integer part of x. Thus,

$$\mathcal{P}_{i,j} \equiv \{(i-k,[j/2^k]): \forall k = 0 \ldots i\}.$$
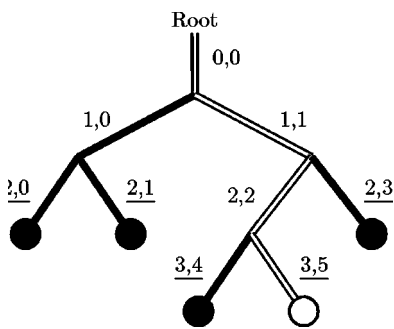

FIG. 7. An example of an asymmetric tree $\mathcal{T}$ consisting of all labeled branches. Circles represent the air sacs connected by the terminal branches (shown with underlined labels) belonging to $\mathcal{L}$. The double line ($=$) shows the path $\mathcal{P}_{3,5}$ connecting the terminal branch $(3,5)$ to the root.
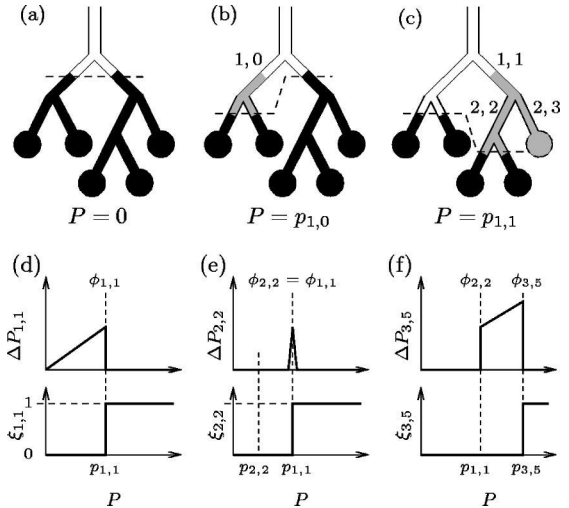

FIG. 8. The process of airway opening in a tree. (a)–(e) show the states of the tree with increasing P. Branches are labeled as shown in Fig. 7. Open branches are shown as outlines, newly opened branches are shown in gray, and closed branches are shown in black. The active surface is shown as a dashed line. Inflation begins at $P=0$ with all branches other than the root closed (a) and proceeds by airway openings, either individually (b) or in an avalanche (c), as P is increased. (d), (e) show the pressure differences ΔP and states ξ of three segments (1,1), (2,2), and (3,5), respectively, belonging to the path $\mathcal{P}_{3,5}$, shown in Fig. 7. Different behavior is observed for branches on the active surface and those embedded in an avalanche.

Each branch is either open or closed. The state (open or closed) of a branch (i,j) is described by a Boolean variable $\xi_{i,j}$ such that

$$\xi_{i,j} \equiv \begin{cases} 0 & \text{if } (i,j) \text{ is closed} \\ 1 & \text{if } (i,j) \text{ is open.} \end{cases}$$

Every branch (i,j) is assigned a threshold pressure $p_{i,j}$. The threshold pressure determines the transition of the branch from a closed to an open state.

1. Airway opening

At the beginning of inflation, the lung is completely degassed and we assume that all airways except the root are closed. Thus, $\xi_{0,0}=1$, and $\xi_{i,j}=0$ otherwise. The pressure in all closed branches of the tree is 0. The external pressure P at the root of the tree is increased from 0 by infinitesimal amounts until all branches in the tree are open. After each increase in P, the system is allowed to reach equilibrium, until all open branches connected to the root are at pressure P.

All closed branches whose parent is also closed do not see any pressure difference ΔP across their length. However, a closed branch (i,j) whose parent is open experiences a pressure difference $\Delta P_{i,j}$. These branches form an interface between the open and closed regions of the lung (dashed line in Fig. 8) called an active surface [41]. Since the equilibrium pressure in the open branches is P and that inside closed branches is 0, $\Delta P_{i,j}=P$. However, transients during airway
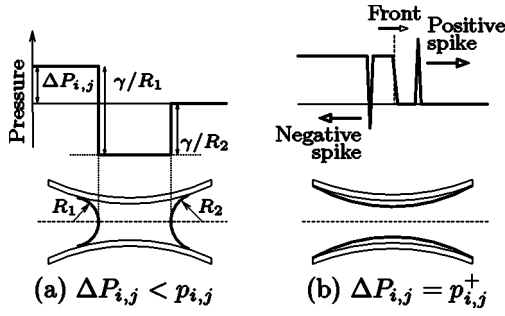
FIG. 9. Pressure along the axis of a liquid bridge in branch (i,j) when $\Delta P_{i,j}$ is just above $p_{i,j}$, the liquid bridge breaks, a pair of sound waves ("crackles") are generated, and the pressure front propagates downstream.

openings could cause $\Delta P_{i,j} > P$ for some branches on the active surface.

Figure 9 illustrates the opening of an airway (i,j) under an applied pressure difference $\Delta P_{i,j}$. For $\Delta P_{i,j} < p_{i,j}$, the liquid bridge in the airway has a finite thickness and the surface tension γ of the liquid is able to sustain the pressure difference [Fig. 9(a)]. When the pressure difference $\Delta P_{i,j}$ across the branch exceeds its threshold pressure $p_{i,j}$, surface tension can no longer sustain the liquid bridge. At this point, the airway opens and the energy stored in the liquid bridge is released in the form of a pair of sound waves (one traveling upstream and the other downstream) called crackles [Fig. 9(b)]. Immediately following opening, the air pressure on two sides of the former liquid bridge is significantly different and the two regions are separated by a sharp pressure front.

The pressure front diffusively propagates deeper into the tree until the two daughters of the branch (i,j) are exposed to the external pressure P (Fig. 9). If the threshold pressures of the daughters are lower than P, the daughters open simultaneously with the parent. The process of opening is continued until all closed branches connected to the root of the tree have threshold pressures greater than P, and a new active surface is formed. The simultaneous opening of a subtree following a small increase in P is called an avalanche [38].

2. Threshold pressures

The threshold pressure of an airway strongly depends on local variables such as the rigidity of the airway walls, the amount of fluid present, and its surface tension [34,35]. Since these quantities vary from airway to airway, the threshold pressures can be effectively considered to be independent random variables distributed according to generation-dependent distribution functions $\rho_i(p)$. Although we allow ρ_i to be generation-dependent, we assume that branches of any given generation are statistically identical and hence their threshold pressures are drawn from the same distribution.

A branch (i,j) is open if and only if it has an open parent and the pressure difference $\Delta P_{i,j} = P$ across it exceeds its threshold pressure $p_{i,j}$. Thus

$$\xi_{i,j} = \Theta(P - p_{i,j}) \ \xi_{i-1,[j/2]}, \tag{11}$$

where

$$\Theta(x) \equiv \begin{cases} 1 & \text{for } x \geq 0, \\ 0 & \text{for } x < 0, \end{cases}$$

is the unit-step function.

3. Opening pressures

Every open branch (i,j) other than the root undergoes a transition from being closed to being open at a pressure defined as the opening pressure $\phi_{i,j}$ of the branch,

$$\xi_{i,j} \equiv \Theta(P - \phi_{i,j}). \tag{12}$$

Using this definition and Eq. (11), we can write $\Theta(P - \phi_{i,j}) = \Theta(P - p_{i,j}) \ \Theta(P - \phi_{i-1,[j/2]})$, which has a solution

$$\phi_{i,j} = \max(p_{i,j}, \phi_{i-1,[j/2]}). \tag{13}$$

Thus the opening pressure $\phi_{i,j}$ of a branch (i,j) is the maximum of its threshold pressure $p_{i,j}$ and the opening pressure of its parent $\phi_{i-1,[j/2]}$.

If the threshold pressure $p_{i,j}$ of a branch (i,j) is less than the opening pressure of its parent $\phi_{i-1,[j/2]}$, the opening pressure $\phi_{i,j} = \phi_{i-1,[j/2]}$ and thus the branch (i,j) and its parent open simultaneously as part of an avalanche. For example, the branch $(2,2)$ opens simultaneously with its parent $(1,1)$ in Figs. 8(c) and 8(e). For a branch (i,j) on the active surface, the threshold pressure $p_{i,j}$ is greater than the opening pressure of its parent $\phi_{i-1,[j/2]}$, since this is precisely the condition that stops an avalanche and produces the active surface. Thus according to Eq. (13), the opening pressure $\phi_{i,j} = p_{i,j}$, which is greater than the opening pressure of its parent, $\phi_{i-1,[j/2]}$. For example, the branch $(3,5)$ does not open simultaneously with its parent $(2,2)$ but at a higher opening pressure [Fig. 8(f)].

4. Transients

The threshold pressures $p_{i,j}$ are assigned *a priori* and represent the quasistatic opening pressures of the airways. However, during fast dynamic openings within an avalanche, the actual threshold pressures and the pressure difference across the segment could be different from their static counterparts. In particular, crackles which accompany airway openings cause an instantaneous increase in ΔP. We therefore replace the step function $\Theta(P - p_{i,j})$ by a more general function $F_{i,j}(P) \equiv F(P, p_{i,j}, \phi_{i-1,[j/2]})$, which is also a step function whose argument depends on the opening pressure of the parent $(i-1,[j/2])$ in addition to the pressure P and the threshold pressure $p_{i,j}$. Thus we rewrite Eq. (11) as

$$\xi_{i,j} = F_{i,j}(P) \xi_{i-1,[j/2]}. \tag{14}$$

The exact form of $F_{i,j}(P)$ depends on the model of airway opening considered.

B. Analytical solution

Equation (14) recursively expresses the state of airway (i,j) in terms of the state of its parent. By iterating Eq. (14), we write the nonrecursive form as

$$\xi_{i,j}=F_{i,j}\ F_{i-1,[j/2]}\cdots F_{0,0}\xi_{0,0}=\prod_{(k,l)\in\mathcal{P}_{i,j}} F_{k,l}(P),\quad (15)$$

since $\xi_{0,0}=1$ as the root is always open. Thus a branch (i,j) is open if and only if all branches along the path $\mathcal{P}_{i,j}$ connecting it to the root of the tree are open.

1. Airway tree partitioning

We can now calculate the fraction of open air sacs at a given pressure. Since each terminal airway subtends one air sac, the total number of air sacs in the lung is equal to n_T, the number of terminal airways. An air sac is open if the terminal airway connected to it is open, and the fraction of open air sacs f_a is given by

$$f_a=\frac{1}{n_T}\sum_{(i,j)\in\mathcal{L}} \xi_{i,j},\qquad (16)$$

where the sum $\Sigma\xi_{i,j}$ gives the number of open leaves of the tree. To compare our results with experimental data, it is necessary to average over all configurations of threshold pressures $p_{i,j}$. Using Eq. (16), the averaged quantity $\langle f_a\rangle$ can be written as

$$\langle f_a\rangle=\frac{1}{n_T}\int \mathcal{D}p\rho(p)\left[\sum_{(i,j)\in\mathcal{L}} \xi_{i,j}\right],\qquad (17)$$

where

$$\int \mathcal{D}p\ \rho(p)\equiv\int_{-\infty}^{\infty}dp_{0,0}\ \rho_0(p_{0,0})\ldots\int_{-\infty}^{\infty}dp_{i,j}\rho_i(p_{i,j})\cdots$$

represents an integration over all possible values of the threshold pressures of every branch in the tree. We note that since the distributions $\rho_i(p_{i,j})$ are normalized, each of the bare integrals $\int dp_{i,j}\ \rho_i(p_{i,j})=1$ and their product $\int Dp\rho(p)=1$. Thus the expression in Eq. (17) is self-normalized. Reversing the order of the commutative operations of integration and summation, we get

$$\langle f_a\rangle=\frac{1}{n_T}\sum_{(i,j)\in\mathcal{L}}\ \int \mathcal{D}p\rho(p)\xi_{i,j},=\frac{1}{n_T}\sum_{(i,j)\in\mathcal{L}} \langle\xi_{i,j}\rangle.$$
$$(18)$$

Thus, Eq. (18) partitions the averaged fraction of open air sacs in the tree into a normalized sum of probabilities of the existence of open paths from the terminal branches to the root of the tree.

2. Opening probabilities

The state variable $\xi_{i,j}$ is a product of terms that are functions of the threshold pressures of all branches along the path $\mathcal{P}_{i,j}$ and the external pressure P, as expressed by Eq. (15).

Since the distribution functions ρ only depend on the generation number, the averaged quantity $\langle\xi_{i,j}\rangle$ depends only on the external pressure P and the generation number i. We define $\Gamma_i(P)\equiv\langle\xi_{i,j}\rangle$, which is the opening probability of a branch (i,j) at pressure P, so Eq. (18) can be rewritten as

$$\langle f_a\rangle=\frac{1}{n_T}\sum_{(i,j)\in\mathcal{L}} \Gamma_i(P).$$

Collecting all terminal branches of the same generation n, we can rewrite the above sum as

$$\langle f_a\rangle=\sum_{n} \Pi(n)\Gamma_n(P),\qquad (19)$$

where $\Pi(n)$ is the distribution of generation numbers n of the terminal branches, i.e., the fraction of terminal branches with generation number n.

Equation (19) conveniently separates the effects of morphological features of the tree structure in a lung, given by the distribution of terminal depths $\Pi(n)$, from the dynamic component described by the opening probability $\Gamma_n(P)$. This allows us to calculate $\Pi(n)$ from models of tree structure and $\Gamma_n(P)$ from models of different dynamical processes in a much simpler geometry.

We note that for a symmetric tree, all terminal branches at the same generation N and thus the generation distribution Π_S of the terminal branches for a symmetric tree is given by

$$\Pi_S(n)=\delta_{n,N}.$$

Using Eq. (19), the fraction of open air sacs $\langle f_a^S\rangle$ for a symmetric tree can be calculated as

$$\langle f_a^S\rangle=\Gamma_N(P).\qquad (20)$$

Thus Eq. (19) allows us to use the results obtained for symmetric trees and translate them to asymmetric trees with different $\Pi(n)$.

3. The P-V curve

We can now write a comprehensive expression for the volume V of the lung as a function of pressure P. Using the expressions of Eqs. (5) and (8) and replacing f_a by $\langle f_a\rangle$, we get

$$V(P)=V_E(P)\ \langle f_a\rangle,$$

which can by expanded using the result of Eq. (19) as

$$V(P)=V_E(P)\sum_{n} \Pi(n)\ \Gamma_n(P).\qquad (21)$$

Although the expression in Eq. (21) was obtained for a binary tree, it is equally applicable to trees of different, even heterogeneous, branching. Thus in Sec. IV we calculate $\Gamma_n(P)$ for various models on linear chains of n generations and apply those results to the asymmetric airway tree.

IV. MODELS OF AIRWAY OPENING

We consider a linear chain of N closed branches labeled $j = 1, \ldots, N$. The internal pressure in the pipe is 0 while an external pressure, P, is applied at one end ($j = 0$). The quantity of interest in this case is $\Gamma_N(P)$, which is defined as the probability of fluid flow in a pipe with N closures at pressure P. For end-to-end fluid flow, we need all the N closures to be open at the given pressure P. At pressure $P = 0$, all closures are closed and hence the probability of flow $\Gamma_N(0) = 0$.

We define a probability density function $\psi_j(\phi)$ such that $\psi_j(\phi)d\phi$ is the probability for closure j to have an opening pressure between ϕ and $\phi + d\phi$. A function $G_j(\phi'|\phi)$ can then be defined as a conditional probability that the branch $(j+1)$ has an opening pressure between ϕ' and $\phi' + d\phi'$, given that the jth closure opens between pressures ϕ and $\phi + d\phi$. This allows us to write

$$\psi_{j+1}(\phi') = \int_0^1 d\phi\, G_j(\phi'|\phi)\psi_j(\phi). \qquad (22)$$

We note that there is a one-to-one correspondence between the conditional probabilities $G(\phi'|\phi)$ and the opening functions $F_{i,j}(P)$. Defining either of these two functions completely defines the dynamics of the system.

To calculate ψ_j, we need an initial state, which can be calculated by defining a hypothetical closure at $j = 0$ and assuming that this closure is permanently open, that is, $\phi_0 = 0$. Thus,

$$\psi_0(\phi) = \delta(\phi). \qquad (23)$$

The opening probability, $\Gamma_N(P)$, can thus be written as

$$\Gamma_N(P) = \int_0^P d\phi\, \psi_N(\phi). \qquad (24)$$

In the following subsections, we define three specific models of airway openings, construct their respective conditional probabilities $G(\phi'|\phi)$, and calculate the opening probability $\Gamma_N(P)$. The first, model A, describes the simplest process of avalanching. Models B and C add the effect of transients, especially crackles, to the opening process by modifying the threshold pressures of the segments permanently or temporarily. Pressures are normalized such that the maximum threshold pressure P_0 in the tree is 1. In all three models we assume that the threshold pressure distribution $\rho(p)$ is uniform between 0 and 1. These models then allow us to fit the experimental P-V curve using Eq. (21).

A. Model A: Simple avalanching

This is the simplest model of airway opening. To construct $G(\phi'|\phi)$, we look at the processes by which a branch opens. If the opening pressure ϕ' of the $(j+1)$th branch is less than that of the jth branch, ϕ, the branch $(j+1)$ will open simultaneously with the branch j as a part of an avalanche. We could thus write G for this part as $\phi\delta(\phi'-\phi)$, where the factor ϕ is numerically the probability that ϕ' is less than ϕ, since the distribution of threshold pressures is

uniform. The δ function reflects the fact that the $(j+1)$th branch opens at the same pressure as the jth one. However, if ϕ' is greater than ϕ, the $(j+1)$th branch will open independently and G will contain a term $\Theta(\phi'-\phi)$, Θ being the unit step function, reflecting the ordering of the opening pressures. The function G is thus given by

$$G^A(\phi'|\phi) = \phi\delta(\phi'-\phi) + \Theta(\phi'-\phi). \qquad (25)$$

Using Eqs. (23) and (25) and by repeated application of Eq. (22), we find

$$\psi_j^A(\phi) = j\phi^{j-1}. \qquad (26)$$

Thus using Eq. (24), we are able to derive the opening probability as

$$\Gamma_N^A(P) = P^N. \qquad (27)$$

This is identical to the expression in Eq. (1) that can be derived using other methods [26–28].

B. Model B: Permanent effect of pressure wave

In this case we slightly alter the algorithm for the change of state of a closure. In addition to opening only when the pressure across the closure exceeds its threshold pressure, we take into account the added effect of a pressure wave. When closure j opens, a pressure wave is set up in the fluid which facilitates the opening of closure $(j+1)$. We take this into account by changing the opening pressure of the closure $(j+1)$ as

$$\phi_{j+1} \rightarrow \alpha\phi_{j+1}, \qquad (28)$$

where, α (<1) is a constant. In this model, the reduction of the threshold pressure is permanent, i.e., once a parent opens the threshold pressure of the child, it is maintained at the reduced level for the duration of the experiment. Thus for all practical purposes, the threshold pressures of all generations greater than 1 are distributed uniformly between 0 and α while that of the first generation is distributed between 0 and 1 (as it cannot be opened in the wake of the pressure wave from the parent).

We can then modify Eq. (25) to write the function $G^B(\phi'|\phi)$ for model B as

$$G^B(\phi'|\phi) = \frac{\phi}{\alpha}\Theta(\alpha-\phi)\delta(\phi'-\phi) + \frac{1}{\alpha}\Theta(\alpha-\phi')$$

$$\Theta(\phi'-\phi) + \Theta(\phi-\alpha)\delta(\phi'-\phi). \qquad (29)$$

The first term again represents the avalanche part of the closure opening, but in this case the renormalization of the opening (ϕ) increases the probability factor by $1/\alpha$. A step function is also included, which distinguishes the behavior of the closures for pressures less than α from the automatic opening at pressures greater than α. The second term represents the independent opening of a closure and the probability is again rescaled by a factor $1/\alpha$. The two step functions in this term not only reinforce the distinction in the first part,

but also restrict the possible values of ϕ' to less than α. The final term is included to take into account the automatic opening of the closures at pressures greater than α.

Using the result of Eq. (29) in Eq. (22) and the initial condition from Eq. (23), we can derive

$$\psi_j^B(\phi) = j\left(\frac{\phi}{\alpha}\right)^{j-1}\Theta(\alpha-\phi) + \Theta(\phi-\alpha). \qquad (30)$$

Again the fluid flow probability can be derived using Eq. (24) as

$$\Gamma_N^B(P) = P\left(\frac{P}{\alpha}\right)^{N-1}\Theta(\alpha-P) + P\Theta(P-\alpha). \qquad (31)$$

C. Model *C*: Transient effect of pressure wave

The depression of the opening pressure due to the pressure wave in model *B* [Eq. (28)] is a permanent phenomenon. This means that once the threshold is lowered by the pressure wave, it does not regain its original value. Thus all thresholds after the first one are distributed between 0 and α and not between 0 and 1. However, apart from this renormalization, there is very little that is different between models *A* and *B*. We shall now try to explore a more intricate model in which the reduction of opening pressure is only a temporary phenomenon and the threshold regains its original value after a short time, unless the closure is opened instantly. We shall deal only with instantaneous reduction of the threshold, which facilitates the avalanchelike opening of the closure but has no effect on the independent change of state.

The conditional probability $G^C(\phi'|\phi)$ for this model is given by

$$G^C(\phi'|\phi) = \frac{\phi}{\alpha}\Theta(\alpha-\phi)\delta(\phi'-\phi) + \Theta(\alpha-\phi)\Theta\left(\phi'-\frac{\phi}{\alpha}\right)$$
$$+ \Theta(\phi-\alpha)\delta(\phi'-\phi). \qquad (32)$$

As mentioned earlier, the process of avalanching in this model is identical to model *B* and thus the first term of G^C is identical to that in Eq. (29). However, the second term, describing independent opening, is markedly different in this case. Not only is there no rescaling of the opening pressures in this event, there is also the absence of the restricting step function on ϕ'. Thus ϕ' can now take values greater than α and give rise to delayed large avalanches. The final term is again identical to that in Eq. (29). This is because at pressures greater than α all closures are opened in large avalanches.

Equation (32) can now be used to solve for the probability density function, $\psi_j^C(\phi)$, which is given by

$$\psi_j^C(\phi) = A_j(\alpha)\phi^{j-1}\Theta(\alpha-\phi)$$
$$+ \left[1 + \sum_{k=1}^{j-1} B_k(\alpha)\phi^k\right]\Theta(\phi-\alpha), \qquad (33)$$
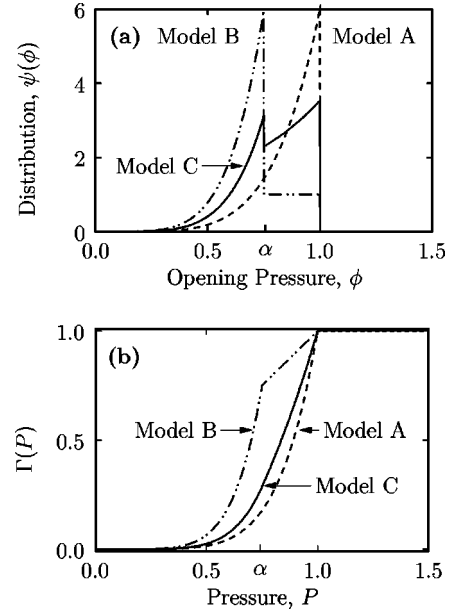
where

FIG. 10. (a) The distribution $\psi(\phi)$ of opening pressures ϕ and (b) the opening probability $\Gamma(P)$ of an airway as obtained from the three models of airway opening (*A*, *B*, and *C*) for a chain of six branches and with $\alpha = 0.75$ for models *B* and *C*.

$$A_j(\alpha) = \prod_{k=1}^{j}\left(\frac{1}{\alpha} + \frac{\alpha^k}{k}\right),$$

$$B_j(\alpha) = A_{j-1}(\alpha)\left(\frac{\alpha^j}{j}\right) \qquad (34)$$

for $j \geq 1$, and $A_0(\alpha) = B_0(\alpha) = 1$.

Upon integrating Eq. (33) with respect to ϕ, we get

$$\Gamma_N^C(P) = A_{N-1}(\alpha)\left(\frac{P^N}{N}\right)\Theta(\alpha-P) + \Gamma_N^{C>}(P)\Theta(P-\alpha), \qquad (35)$$

where

$$\Gamma_N^{C>}(P) = B_N(\alpha) + \sum_{k=0}^{N-1}\frac{B_k(\alpha)}{k+1}(P^{k+1} - \alpha^{k+1}). \qquad (36)$$

The opening probability Γ_N and the distribution ψ of opening pressures ϕ for the three models are compared in Fig. 10. The distribution ψ for model *C* [Fig. 10(a)] is visually similar to the distributions obtained from experimental data (Fig. 5). We note that Γ_N is identical to the open fraction in a symmetric tree [Eq. (20)]. Thus for the same maximum threshold pressure and number of generations, models *B* and *C* recruit more air sacs than the simple avalanching model *A* [Fig. 10(b)].

We can construct more sophisticated models of airway opening by extending these basic models. The pressure wave could have a partly instantaneous and partly permanent effect on ϕ by combining models *B* and *C*. The parameter α could be distributed instead of being a fixed number. The threshold pressure distributions could be made nonuniform as well as

generation-dependent. In each case, the technique described in this section could be used to obtain an analytical solution for $\psi(\phi)$ and $\Gamma_N(P)$. These results can then be combined with a distribution of generation numbers of terminal branches $\Pi(n)$ and the elastic P-V curve $V_E(P)$ to obtain the final pressure-volume relationship of the lung.

V. FITTING EXPERIMENTAL DATA

We fit the $f_v(P)$ curves obtained from experimental data (Fig. 4) with polynomial functions $\Sigma_n a_n(P/P_0)^n$ up to the inflection point $P_\times$ in the curves. The maximum threshold pressure P_0 is given by the pressure above which all branches are open and thus $f_v=1$. The inflection points in the curves are determined by numerically differentiating the curves for f_v and finding the first maxima. For model A, we determine P_0 by fitting the curve up to $P_\times$ and extrapolating it to $f_v=1$. For model C, $P_\times$ represents the point of crossover from avalanchelike behavior to pressure-wave mediated behavior and thus the parameter $\alpha=P_\times/P_0$.

We use polynomials of order 48, since this is the known maximum depth in a dog lung [32]. The large number of coefficients makes simple regression unstable, and we use an additive diagonal term in the coefficient matrix to regularize the results. The raw fit thus obtained is then fine-tuned by randomly updating each coefficient by a small amount and recalculating the fitting errors simultaneously in the normal and logarithmic scales, to ensure the accuracy of the coefficients for small n.

For model A, f_v is given by using Eqs. (19) and (27) as

$$\langle f_v^A \rangle = \sum_n \Pi(n) \left(\frac{P}{P_0} \right)^n \tag{37}$$

and the coefficients of the fitted polynomial $a_n=\Pi(n)$, the distribution of terminal generations. For model B, the expression for f_v for pressures less than α is given by

$$\langle f_v^B \rangle = \sum_n \frac{\Pi(n)}{\alpha^{n-1}} \left(\frac{P}{P_0} \right)^n \tag{38}$$

and the distribution can be calculated from the polynomial fit as $\Pi(n)=a_n\alpha^{n-1}$. Similarly, for model C, the f_v is given by

$$\langle f_v^C \rangle = \sum_n \Pi(n) \frac{A_n(\alpha)}{n} \left(\frac{P}{P_0} \right)^n \tag{39}$$

for pressures up to α. Thus, the distribution of generation numbers of the terminal segments can be estimated by $\Pi(n)=na_n/A_n(\alpha)$.

For models B and C, we fit the region $P>\alpha$ using the expressions for $\Gamma_n(P)$ in this region as given by Eqs. (31) and (35) and the same $\Pi(n)$ as obtained by fitting the region $P<\alpha$. The fitted curves for f_v using models A and C for lobe A are displayed in Fig. 11(a). The distribution $\Pi(n)$ obtained using model C is shown in Fig. 11(b).

The distribution $\Pi(n)$ in Fig. 11(b) has two distinct regions, a narrow peak for $n<5$ (shown as open rectangles)
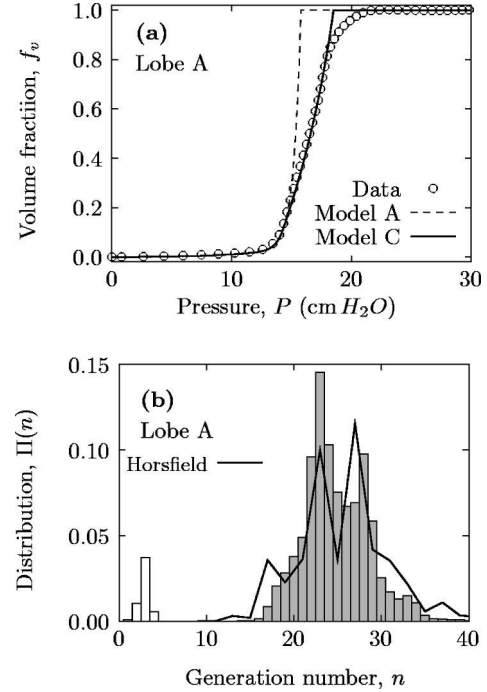

FIG. 11. (a) The volume fraction f_v of the open air sacs obtained using models A and C obtained by fitting the experimental data for lobe A and (b) the distribution $\Pi(n)$ of the generation numbers n of the terminal branches obtained from the fit, compared to the distribution for the Horsfield model of the dog lung.

and a broad distribution for $15<n<40$ (shown as filled rectangles). The second part of the distribution has two main peaks in the region $22<n<30$.

We compare $\Pi(n)$ to a known model for the airway tree structure, the Horsfield model [32], which is an asymmetric self-similar description of averaged experimental data obtained by physical measurements on a polymer cast of the airway tree. The Horsfield distribution corresponds in shape and position with the $\Pi(n)$ obtained by fitting the P-V data. We are able to recover the two main peaks at approximately their correct positions. The small-n part of the distribution ($n<5$) that we obtain from our data does not correspond to the branching structure of the tree since the dog lung is not known to have terminals with depths $n<13$.

We attribute the existence of the small-n part of $\Pi(n)$ to the airway wall elasticity and the volume of air contained in the airways before any air sacs open (Appendix A). The first few branches of the airway tree are held open by cartilaginous rings, and the expansion of these branches at low P also contributes to the small-n part of $\Pi(n)$. We ignore this region when focusing on the branching structure and normalize the Horsfield model to only the area under the second part of the distribution. The Horsfield model is an idealized description of the dog lung and does not account for the differences between individual dogs. In contrast, with our approach we can also identify the variation in structure among specific samples.

Finally, using Eq. (5), we combine the effect of elasticity to obtain the full P-V curves of our models using the expres-
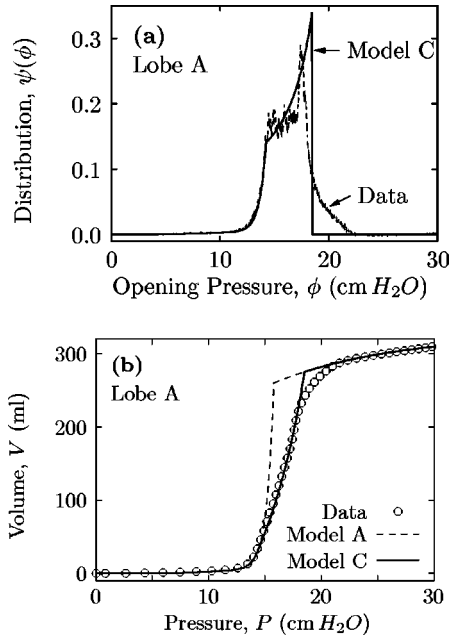
FIG. 12. (a) The distribution $\psi(\phi)$ of opening pressures ϕ using model C compared to the experimental data from lobe A and (b) the full P-V curve reconstructed using Eq. (3) and model C, compared to the experimentally obtained data.

sion for $V_E(P)$ from Eq. (4) along with the parameters obtained from the fits shown in Fig. 3. Figure 12(a) compares the distribution of opening pressures using model C with that obtained using the experimental data. The resulting P-V curves are compared in Fig. 12(b).

The P-V curve of model C has a small deviation from the experimental curve near the maximum threshold pressure [Fig. 12(b)] due, we believe, to an underestimation of the maximum threshold pressure, i.e., the pressure at which all airways are opened. Our assumption that the maximum threshold pressure of the branches corresponds to the pressure at the point of inflection is only true when the distribution of threshold pressures is uniform and generation-independent. However, if the threshold pressures are generation-dependent, our method underestimates the maximum threshold pressure [27,48]. To estimate the effect of generation dependence, we simulated inflation of randomly branched trees using a simple generation-dependent threshold pressure distribution with overlapping domains. We found that the inflection point shifts to a pressure smaller than the maximum threshold pressure, independent of the exact distribution or the degree of randomness in branching. The high pressure in this region would allow a more significant contribution from the opening of the deeper air sacs [Eq. (21)], which we are unable to probe accurately. However, in real lungs, these air sacs ($n > 30$) are few in number [Fig. 11(b)] and do not contribute significantly to the shape of the P-V curve.

VI. CONCLUSION

In conclusion, we have derived a general theory for quasistatic fluid flow through collapsible bifurcating structures.

We show that while calculating the pressure-volume curve or analogous average descriptions of fluid transport, the complex branching structure can be partitioned into a linear superposition of one-dimensional chains. Using this result we constructed a comprehensive model of the lung P-V curve based on the topology of the lung airway tree, the elasticity of the lung tissue, and the mechanisms of airway openings. We have shown that transient pressure waves during the process of airway openings significantly affect the shape of the P-V curve. Although the full P-V curve is a result of the combination of influences, we have been able to separate the effect of each of these factors using a single measurement. The resulting method also provides an estimate of the distribution of the generation number of the terminal branches in the airway tree, or the depth of the air sacs in the lung. Since the estimated distributions compare favorably to available morphological data, our approach should be useful in clinical situations as well as in developmental studies. In general, our results, particularly those involving tree partitioning and the general solution of the opening process, are equally applicable to other physical systems involving transport in asymmetrically branched structures.

APPENDIX A: VOLUME OF AIRWAYS

We can calculate the contribution of airways to the total volume of the lung using Eq. (19). Assuming each airway is a cylinder whose radius r_i and length ℓ_i are exponential functions of generation number i [1],

$$r_i = \beta^i r_0, \tag{A1a}$$

$$\ell_i = \gamma^i \ell_0, \tag{A1b}$$

the volume of an airway (i, j) can be written as

$$v_i = \pi r_i^2 \ell_i = \kappa^i v_0, \tag{A2}$$

where $\kappa = \beta^2 \gamma$ and v_0 is the volume of the root branch. For a symmetric tree, there are 2^i branches at the ith generation and the opening probability of each of them is $\Gamma_i(P)$. Assuming that the elasticity of airways is identical to that of air sacs, the averaged total volume V_b of open airways is thus given by

$$V_b \propto V_E(P) \sum_n 2^n v_n \Gamma_n(P) \propto V_E(P) v_0 \sum_n (2\kappa)^n \Gamma_n(P). \tag{A3}$$

If $2\gamma < 1$, most of the contributing volume to V_b comes from the small n region where the branching is symmetric. The maximum airway volume $V_{b,\max}$ can be approximated as that V_b for an infinite tree with all branches open. Thus,

$$V_{b,\max} \propto \frac{v_0}{1 - 2\kappa} V_0. \tag{A4}$$

Thus the relative volume of the airways is given by

$$\frac{V_b}{V_{b,\max}} = (1 - 2\kappa) \frac{V_E(P)}{V_0} \sum_n (2\kappa)^n \Gamma_n(P). \tag{A5}$$

We note that if the volume of air sacs V_b is allowed to contribute to the total volume of the lung $V(P)$, the terms in the expansion with respect to Γ_n decay exponentially and are only significant for small values of n, as can be seen from the open boxes in Fig. 11(b).

---

[1] M.F. Shlesinger and B.J. West, Phys. Rev. Lett. **67**, 2106 (1991).

[2] H.J. Herrmann, Phys. Rep. **136**, 153 (1986).

[3] H. Takayasu, *Fractals in the Physical Sciences* (Manchester University Press, Manchester, 1990).

[4] P. Prusinkiewicz and A. Lindenmayer, *The Algorithmic Beauty of Plants* (Springer Verlag, New York, 1990).

[5] *Fractals in Natural Sciences*, edited by T. Vicsek, M. Shlesinger, and M. Matsushita (World Scientific, Singapore, 1994).

[6] J.B. Bassingthwaighte, L.S. Liebovitch, and B.J. West, *Fractal Physiology* (Oxford University Press, New York, 1994).

[7] R.E. Collins, *Flow of Fluids Through Porous Media* (Pennwell, Tulsa, OK, 1961).

[8] S. Kirkpatrick, Rev. Mod. Phys. **45**, 574 (1973).

[9] A.E. Scheidegger, *The Physics of Flow Through Porous Media*, 3rd ed. (University of Toronto, Toronto, 1974).

[10] *Dynamics of Fluids in Hierarchical Porous Media*, edited by J. H. Cushman, (Academic, San Diego, 1990).

[11] D. Stauffer and A. Aharony, *Introduction to Percolation Theory*, 2nd ed. (Taylor and Francis, London, 1992).

[12] P.M. Adler, *Porous Media: Geometry and Transport* (Butterworth-Heinemann, Stoneham, MA, 1992).

[13] M.B. Isichenko, Rev. Mod. Phys. **64**, 961 (1992).

[14] A. Bejan and M.R. Errera, Fractals **5**, 685 (1997).

[15] N. Dan and A. Bejan, J. Appl. Phys. **84**, 3042 (1998).

[16] A. Bejan, *Shape and Structure, From Engineering to Nature* (Cambridge University Press, Cambridge, UK, 2000).

[17] C.P. Bachas and B.A. Huberman, Phys. Rev. Lett. **57**, 1965 (1986).

[18] N. Vandewalle and M. Ausloos, Phys. Rev. E **55**, 94 (1997).

[19] J.S. Andrade, Jr., A.M. Alencar, M.P. Almeida, J.M. Filho, S.V. Buldyrev, S. Zapperi, H.E. Stanley, and B. Suki, Phys. Rev. Lett. **81**, 926 (1998).

[20] M.P. Almeida, J.S. Andrade, Jr., S.V. Buldyrev, F.S.A. Cavalcante, H.E. Stanley, and B. Suki, Phys. Rev. E **60**, 5486 (1999).

[21] D. MacDonald, *Blood Flow in Arteries* (Williams & Wilkins, Baltimore, MD, 1974).

[22] J.H. Bates, J. Appl. Physiol. **75**, 2493 (1993).

[23] C.A. Dawson, G.S. Krenz, K.L. Karau, S.T. Haworth, C.C. Hanger, and J.H. Linehan, J. Appl. Physiol. **86**, 569 (1999).

[24] R.H. Ingram, Jr. and T.J. Pedley, *Handbook of Physiology. The Respiratory System. Mechanics of Breathing* (Am. Physiol. Soc., Bethesda, MD, 1986).

[25] A.B.H. Crawford, D.J. Cotton, M. Paiva, and L.A. Engel, J. Appl. Physiol. **66**, 2511 (1989).

[26] A.-L. Barabasi, S. Buldyrev, H.E. Stanley, and B. Suki, Phys. Rev. Lett. **76**, 2192 (1996).

[27] M.K. Sujeer, S.V. Buldyrev, S. Zapperi, J.S. Andrade, Jr., H.E. Stanley, and B. Suki, Phys. Rev. E **56**, 3385 (1997).

[28] B. Suki, J.S. Andrade, Jr., M.F. Coughlin, D. Stamenović, H.E. Stanley, M. Sujeer, and S. Zapperi, Ann. Biomed. Eng. **26**, 608 (1998).

[29] A.M. Alencar, S.P. Arold, S.V. Buldyrev, A. Majumdar, D. Stamenović, H.E. Stanley, and B. Suki, Nature (London) **417**, 809 (2002).

[30] A. Majumdar, A.M. Alencar, S.V. Buldyrev, Z. Hantos, H.E. Stanley, and B. Suki, Phys. Rev. Lett. **87**, 058102 (2001).

[31] K. Horsfield, Respir. Physiol. **26**, 173 (1976).

[32] K. Horsfield, W. Kemp, and S. Phillips, J. Appl. Physiol.: Respir., Environ. Exercise Physiol. **52**, 21 (1982).

[33] L.A. Engel, A. Grassino, and N.R. Anthonisen, J. Appl. Physiol. **38**, 1117 (1975).

[34] D.R. Otis, Jr., M. Johnson, T.J. Pedley, and R.D. Kamm, J. Appl. Physiol. **75**, 1323 (1993).

[35] D.R. Otis, Jr., F. Peták, Z. Hantos, J.J. Fredberg, and R.D. Kamm, J. Appl. Physiol. **80**, 2077 (1996).

[36] D.P. Gaver, III, R.W. Samsel, and J. Solway, J. Appl. Physiol. **69**, 74 (1990).

[37] P.T. Macklem, D.F. Proctor, and J.C. Hogg, Respir. Physiol. **8**, 191 (1970).

[38] B. Suki, A.L. Barabasi, Z. Hantos, F. Peták, and H.E. Stanley, Nature (London) **368**, 615 (1994).

[39] P. Forgacs, Lancet **2**, 203 (1967).

[40] A.M. Alencar, Z. Hantos, F. Peták, J. Tolnai, T. Asztalos, S. Zapperi, J.S. Andrade, Jr., S.V. Buldyrev, H.E. Stanley, and B. Suki, Phys. Rev. E **60**, 4659 (1999).

[41] A.M. Alencar, S.V. Buldyrev, A. Majumdar, H.E. Stanley, and B. Suki, Phys. Rev. Lett. **87**, 088101 (2001).

[42] J.C. Smith and D. Stamenović, J. Appl. Physiol. **60**, 1341 (1986).

[43] E. Salazar and J.H. Knowles, J. Appl. Physiol. **19**, 97 (1964).

[44] H.J.H. Colebatch, C.K.Y. Ng, and N. Nikov, J. Appl. Physiol.: Respir., Environ. Exercise Physiol. **46**, 337 (1979).

[45] R.K. Lambert, T.A. Wilson, R.E. Hyatt, and J.R. Rodart, J. Appl. Physiol.: Respir., Environ. Exercise Physiol. **52**, 44 (1982).

[46] P.S. Haber, H.J.H. Colebatch, C.K.Y. Ng, and I.A. Greaves, J. Appl. Physiol.: Respir., Environ. Exercise Physiol. **54**, 837 (1983).

[47] M. Amato *et al.*, N. Engl. J. Med. **338**, 347 (1998).

[48] B. Jonson, J.C. Richard, C. Straus, J. Mancebo, F. Lemaire,

and L. Brochard, Am. J. Respir. Crit. Care Med. **159**, 1172 (1999).

[49] B. Suki, A.M. Alencar, M.K. Sujeer, K.R. Lutchen, J.J. Collins, J.S. Andrade, Jr., E.P. Ingenito, S. Zapperi, and H.E. Stanley, Nature (London) **393**, 127 (1998).

[50] R.D. Hubmayr, Am. J. Respir. Crit. Care Med. **165**, 1647 (2002).

[51] P. Pelosi, M. Goldner, A. McKibben, A. Adams, G. Eccher, P. Caironi, S. Losappio, L. Gattinoni, and J.J. Marini, Am. J. Respir. Crit. Care Med. **164**, 122 (2001).

[52] J.W. Essam and M.E. Fischer, Rev. Mod. Phys. **42**, 272 (1970).

[53] N. Deo, *Graph Theory with Applications to Engineering and Computer Science* (Prentice-Hall, Englewood Cliffs, NJ, 1974).